

Method for Detecting an Open Switch Fault in a Grid Connected Npc Inverter System

B.Vishnuvardha & K.Mahender

ABSTRACT: In this paper we are implementing a three level converter which is utilized as the power converter of wind turbine due to its advantage like high efficiency, low collector emitter voltage and low current total harmonic distortion. According to the interior permanent magnet synchronous generator it has the better size and efficiency. Therefore according to the wind turbine system which consist of the three level converter and IPMSG and fault tolerant control for the open circuit fault of switches which is used to improve the reliability. Therefore according to the paper which is perform on the open circuit fault of the outer switches in the three level rectifiers which is connected to the IPMSG .according to the effect ofSx1 andSx4 open-circuit faults have been analysis which is based upon the proposed in the tolerant control. Therefore according to the proposed tolerant control which is maintain in normal operation such as sinusoidal control which is under the open fault of the outer switches by adding a compensation value to the reference voltages. By using the simulation result we can analysis the performance of the proposed system.

I. INTRODUCTION

The power capacity of a wind turbine system has been increasing consistently, leading to the development of generators with large power capacity [1]–[3]. There are many types of generators. Permanent magnet synchronous generators (PMSGs) have high efficiency and high reliability compared with induction generators. This is because external excitation is not required and there are no copper losses in the rotor circuits. Moreover, because of the smaller size of the PMSG, the weight of the wind turbine is reduced [4].

Among various PMSGs, interior PMSGs (IPMSGs) are especially advantageous from the standpoints of efficiency and power generation owing to the use of the reluctance torque [4]–[7]. Generators requiring high voltage need to use multilevel converter topologies to reduce the collector–emitter voltage per switch. Among multilevel topologies, three-level topologies such as the three-level neutral-point clamped (3L-NPC) and T-type topologies are applied in wind turbine systems with a wide power range.

Furthermore, the three-level topology guarantees high efficiency and low-current total harmonic distortion (THD) in comparison with the twolevel topology [8]–[11]. The 3L-NPC topology is vulnerable to switch faults because many switches are used. Switch fault detection and tolerant control

methods for switch faults should be implemented to improve the reliability of wind turbine systems. Switch faults are divided into a short-circuit fault and an open-circuit fault [12]. The short-circuit fault normally leads to a breakdown of the entire system; therefore, fault detection and tolerant control methods for the short-circuit fault require additional circuits. On the other hand, the open-circuit fault leads to current distortion, which can lead to a breakdown if it persists for a long time; therefore, the open-circuit fault should be detected, and the tolerant controls are necessary [9], [12]–[15]. In wind turbine systems, a back-to-back converter is used to transfer power from the generator to the grid. A back-to-back converter using the 3L-NPC topology is shown in Fig. 1.

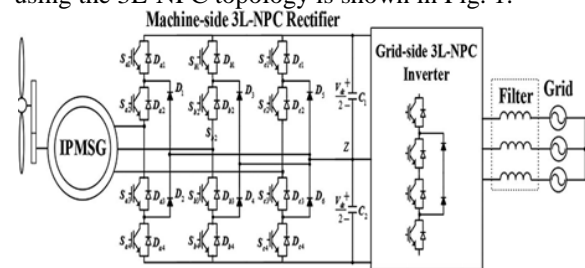


Fig. 1. Back-to-back converter using the 3L-NPC topology in wind turbine systems.

This consists of the machine-side 3L-NPC rectifier, the dc-link, and the grid-side 3L-NPC inverter. Depending on the operating conditions, tolerant controls can be applied for the rectifier or the inverter because the current paths of the rectifier and the inverter are different [9], [13]–[15]. In addition, the different structure of the three-level topologies should be considered in the tolerant controls [9], [13]. In the 3L-NPC inverter, the open-circuit fault of the inner switch causes the outer switch connected it to be infeasible; therefore, changing only the switching method does not become a solution for the open-circuit fault, and the additional devices such as fuses and switches should be added for achieving the tolerant operation under the open-circuit fault of the inner switch.

However, the open-circuit fault of the outer switch can be handled by changed the switching method in limited range [19]. In [19], the tolerant control method limits the output voltage range by half. In the 3L-NPC rectifier, the current distortion caused by the open-circuit fault of the inner switch can be restored partially by clamping the switching

state without any additional devices [14]. In addition, the reactive current is injected to eliminate current distortion caused by the open-circuit fault of the outer switch [22]. This method can also be applied for the T-type rectifier. The T-type rectifier is advantageous on the tolerant control because the switches in a leg are independent of each other. Many tolerant control methods for the open-circuit fault of the inner switch, which can be used in both the T-type inverter and rectifier, were proposed. However, according to the specification of the PMSG, an open-circuit fault of the outer switch can cause current distortion as much as when an open circuit fault of the inner switch occurs [22]. Rectifiers with IPMSGs can operate to generate maximum power at power factor other than unity. IPMSGs provide more power

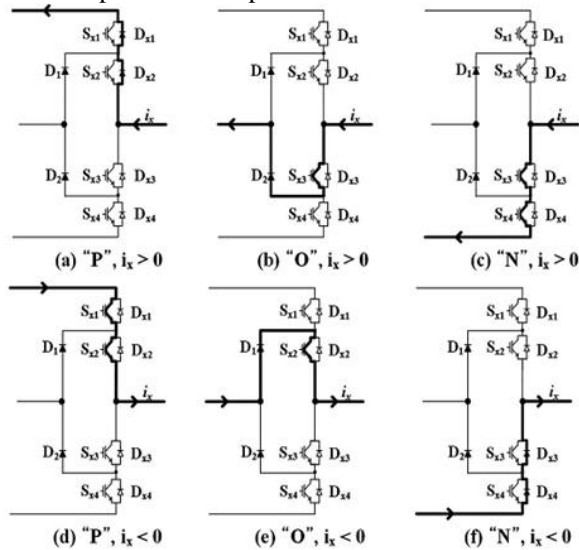
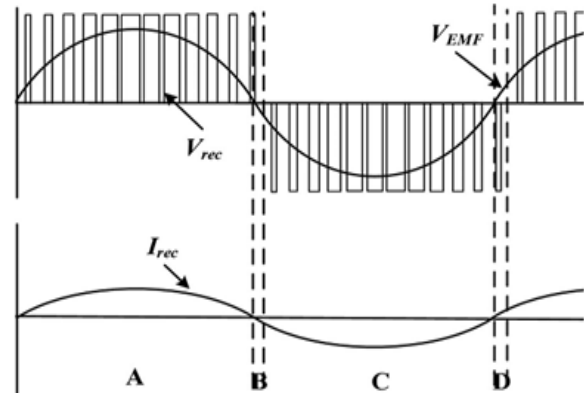


Fig. 2. Current paths depending on the current direction and the switching state.

when rectifiers operate at a unique power factor [4]–[7]. In such a case, an open-circuit fault of the outer switches (S_{x1} and S_{x4}) causes current distortion and torque fluctuation, which can lead to vibration of the wind turbine. In this paper, the reason for the current distortion caused by the outer switches (S_{x1} and S_{x4}) is analyzed, and then, on the basis of this analysis, a tolerant control for S_{x1} and S_{x4} open-circuit faults is proposed. In the proposed tolerant control, the switch with an open-circuit fault is not used to generate the input voltages of the three-level rectifier by adding a compensation value to the reference voltages. The compensation value is simply calculated and the power factor does not change in the proposed tolerant control.

III. OPEN-CIRCUIT FAULT ANALYSIS OF OUTER SWITCHES

There are three switching states (P, N, and O) in the 3L-NPC rectifier [9]. Six current paths can be generated depending on the current direction and the switching state, and these are shown in Fig. 2 [23]. Fig. 3 shows the input current generation process of a rectifier with unity power factor. The rectifier current is I_{rec} , the rectifier voltage is V_{rec} , and the back electromotive force (EMF) is V_{EMF} .



[Figs. 2(a), (b)] [Figs. 2(d), (e)] [Figs. 2(e), (f)] [Figs. 2(b), (c)]

Fig. 3. Rectifier operation at unity power factor.

TABLE I
CURRENT PATH COMPOSITION DEPENDING ON THE PART OF FIG. 3

Part	V_{rec}	I_{rec}	Current path
A	Positive	Positive	(a) P switching state, (b) O switching state (valid)
B	Positive	Negative	(d) P switching state (valid), (e) O switching state
C	Negative	Negative	(e) O switching state (valid), (f) N switching state
D	Negative	Positive	(b) O switching state, (c) N switching state (valid)

The phase difference between V_{EMF} and V_{rec} , which causes the current flow, is controlled to match the phase of I_{rec} up with the phase of the corresponding V_{EMF} . One period of I_{rec} can be divided into four parts depending on the polarity of I_{rec} and V_{rec} . The generated current paths are different depending on the part, and these are summarized in Table I. In parts A and C, the O switching state causes the input current flow; therefore, this is called the valid switching state.

In parts B and D, the P and N switching states are the valid switching state where the current flows through the switches. When the rectifier operates with unity power factor, parts A and C are large, and parts B and D are small. If parts B and C are very small as much as be ignored, the S_{x1} and S_{x4} open-circuit faults can be ignored [22], [23].

In this paper, the other case (Case II), which is the reactive current injection for IPMSG, is also considered. Fig. 4 shows that the input current generation process of the rectifier for Cases I and II. There are two phase differences: the phase difference (ϕ_Z) between V_{EMF} and V_{rec} explained in [22], and

the phase difference (ϕ_{pf}) between I_{ref} and V_{EMF} caused by the ϕ_{pf} . In Fig. 4, part B (or part D) consists of ϕ_Z and ϕ_{pf} , and their lengths increase. This means that the current can be more distorted by the open-circuit fault of the outer switches compared to when ϕ_Z alone is considered

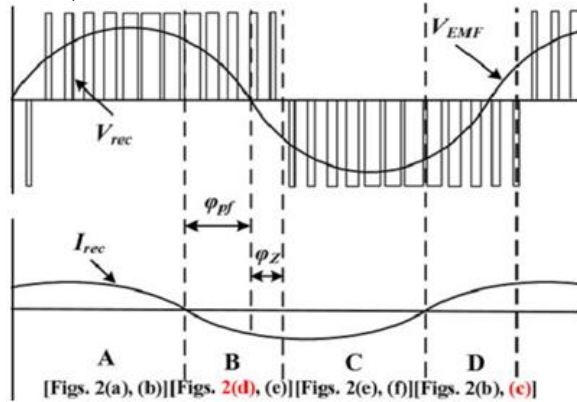


Fig. 4. Rectifier operation at any pf.

Case I can be ignored because ϕ_Z is determined depending on the operating condition of the rectifier and the PMSG. However, because ϕ_{pf} is determined by the pf, Case II should be considered when the IPMSG is employed. The current distortion caused by the open-circuit fault of the outer switches is shown in Fig. 5 for various pfs. Owing to the infeasible open-circuit fault switch, the current becomes zero during the range consisting of ϕ_Z and ϕ_{pf} . The S_{x1} open-circuit fault makes the current path of Fig. 2(d) infeasible.

The current path of Fig. 2(d) belongs to part B; therefore, the S_{x1} open-circuit fault causes distortion in the negative current as shown in Fig. 5(a) and (c). On the contrary, the S_{x4} open-circuit fault leads to distortion in the positive current as shown in Fig. 5(b) and (d) because the current path of Fig. 2(c) related to the S_{x4} open-circuit fault belongs to part D.

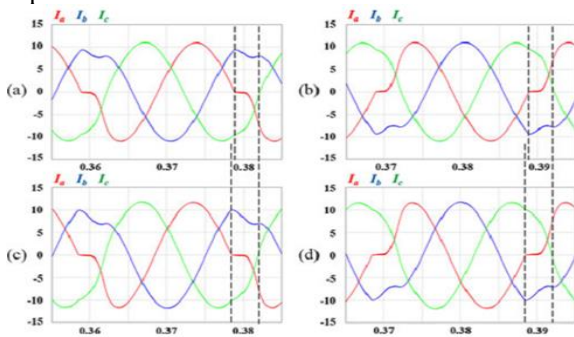


Fig. 5. Current distortion depending on the open-circuit fault and the pf: (a)

0.95pf, S_{x1} open-circuit fault, (b) 0.95pf, S_{x4} open-circuit fault, (c) 0.9pf, S_{x1} open-circuit fault, and (d) 0.9pf, S_{x4} open-circuit fault

III. TOLERANT CONTROL FOR OPEN-CIRCUIT FAULT OF OUTER SWITCHES

An existing tolerant control method for the open-circuit fault of the outer switches is reactive current injection [22]. This method changes the phase of V_{ref} so that it corresponds with the phase of V_{rec} . This means that parts B and D are eliminated. However, this tolerant control method has the disadvantage of low-power generation efficiency of the generator because the PMSG has efficient operating condition which depends on the pf of the rectifier. In general, the unity pf is required for the best operating condition of a surface PMSG. The rectifier voltage (V_{rec}) without the current path related to the open-circuit fault switch is generated by changing the reference voltages. To explain the proposed tolerant control, the S_{x1} open-circuit fault is used as an example.

A. Compensation Voltage (V_{comp}) Calculation

Three-phase reference voltages ($V_{x,ref}$, $x=a, b, c$) are expressed as

$$\begin{aligned} V_{a,ref} &= V_{mag} \cos(2\pi f_s t) \\ V_{b,ref} &= V_{mag} \cos(2\pi f_s t - 2\pi/3) \\ V_{c,ref} &= V_{mag} \cos(2\pi f_s t + 2\pi/3) \end{aligned} \quad (1)$$

where V_{mag} is the magnitude of the reference voltages, and f_s is the fundamental frequency. The offset voltage (V_{offset}) is added to each reference voltage to expand the range of the modulation index ($M_a = \sqrt{3} \times V_{mag}/V_{dc}$). V_{offset} and the changed reference voltages ($V_{x,ref,offset}$, $x=a, b, c$) are expressed as

$$V_{offset} = -(V_{ref,max} + V_{ref,min})/2 \quad (2)$$

$$V_{a,ref,offset} = V_{a,ref} + V_{offset}$$

$$V_{b,ref,offset} = V_{b,ref} + V_{offset}$$

$$V_{c,ref,offset} = V_{c,ref} + V_{offset} \quad (3)$$

Where $V_{ref,max}$ and $V_{ref,min}$ are the maximum and minimum values of $V_{a,ref}$, $V_{b,ref}$, and $V_{c,ref}$. The reference voltages of (3) are compared with the carrier signals to generate V_{rec} . When the S_{x1} open-circuit fault occurs, the current path of Fig. 2(d) should be eliminated to prevent current distortion; therefore, the reference voltage should be changed to generate V_{rec} without the current path of Fig. 2(d). In the proposed tolerant control, a reference voltage of a phase containing the S_x

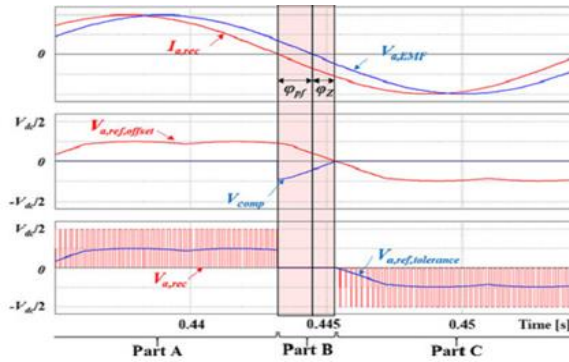


Fig. 6. Change of reference voltages in the proposed tolerant control for the Sx1 open-circuit fault (0.95pf).

open-circuit fault is changed to zero as shown in Fig. 6. As a result, the current path of Fig. 2(d) disappears because the O switching state is only used in part B. To make the reference voltage zero, $|V_{comp}|$ is assigned the magnitude of the reference voltage ($V_{x,ref,offset}$) containing the open-circuit fault, and V_{comp} can be expressed as

$$V_{comp} = -V_{x,ref,offset} \quad (x = a \text{ phase containing open circuited fault switch}) \quad (4)$$

The proposed tolerant control is implemented by adding V_{comp} to the reference voltages ($V_{x,ref,offset}$, $x=a, b, c$). The new reference voltages ($V_{x,ref,tolerance}$, $x=a, b, c$) of the proposed tolerant control are expressed as

$$\begin{aligned} V_{a,ref,tolerance} &= V_{a,ref,offset} + V_{comp} \\ V_{b,ref,tolerance} &= V_{b,ref,offset} + V_{comp} \\ V_{c,ref,tolerance} &= V_{c,ref,offset} + V_{comp} \end{aligned} \quad (5)$$

B. Compensation Range for Adding V_{comp}

By adding V_{comp} to each reference voltage, the use of the current path related to the open-circuit fault switch will be precluded. To achieve this perfectly, V_{comp} is added for the suitable range and position. The compensation range, which is part B or part D of Fig. 4, consists of ϕ_z and ϕ_{pf} . ϕ_z can be calculated with the equivalent circuit of the PMSG and the three-level rectifier [22]. ϕ_z , which is the phase difference between V_{EMF} and V_{rec} , is expressed as

$$\phi_z = \tan^{-1} \left(\frac{-|I_{rec}| * 2\pi f_s L}{V_{EMF} - |I_{ref}| R} \right) \quad (6)$$

where R and L are the equivalent resistance and inductance of the PMSG, and f_s is the fundamental frequency representing the angular frequency of the PMSG. ϕ_{pf} , which is the phase difference between V_{EMF} and I_{rec} , is related to the pf. ϕ_{pf} can be calculated by the pf and this is

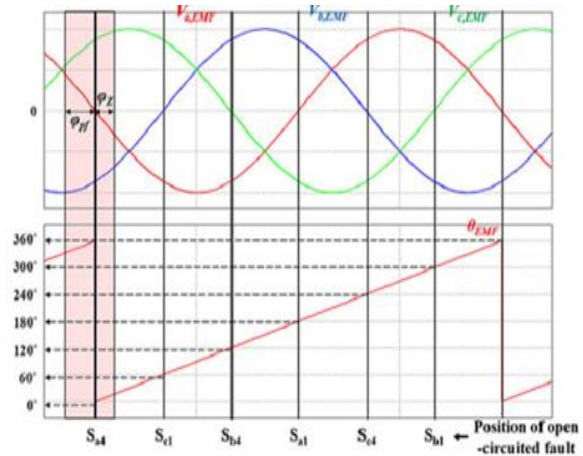


Fig. 7. Compensation position on the basis of VEMF's angle (θ_{EMF}).

TABLE II

Compensation range depending On The position Of The open-Circuit Fault

Position of open-circuit fault	Compensation range
S_{a1}	$(0^\circ - \phi_{pf}) \sim (0^\circ + \phi_z)$
S_{c1}	$(60^\circ - \phi_{pf}) \sim (60^\circ + \phi_z)$
S_{b1}	$(120^\circ - \phi_{pf}) \sim (120^\circ + \phi_z)$
S_{a1}	$(180^\circ - \phi_{pf}) \sim (180^\circ + \phi_z)$
S_{c1}	$(240^\circ - \phi_{pf}) \sim (240^\circ + \phi_z)$
S_{b1}	$(300^\circ - \phi_{pf}) \sim (300^\circ + \phi_z)$

expressed as

$$\phi_{pf} = \cos^{-1}(pf) \quad (7)$$

If the d-q control theorem is used, ϕ_{pf} can be calculated as

$$\phi_{pf} = \cos^{-1} \left(\frac{I_{qe}}{\sqrt{I_{qe}^2 + I_{de}^2}} \right) \quad (8)$$

Where I_{de} indicates the d-axis current related to the flux and I_{qe} indicates the q-axis current related to the torque, and these are values in the d-q synchronous rotating frame. ϕ_z and ϕ_{pf} , which are calculated from (6) and (8), are located near the zero-crossing point of VEMF as shown in Fig. 6. Therefore, the compensation position for adding V_{comp} is defined on the basis of VEMF's angle (θ_{EMF}). Fig. 7 shows three-phase VEMF and θ_{EMF} . θ_{EMF} is acquired from the encoder or position sensor. Six zero-crossing points are expressed for every 60° , which are matched to each open-circuit fault as shown in Fig. 7. Consequently, θ_{EMF} representing each zero-crossing point is a criterion for adding V_{comp} .

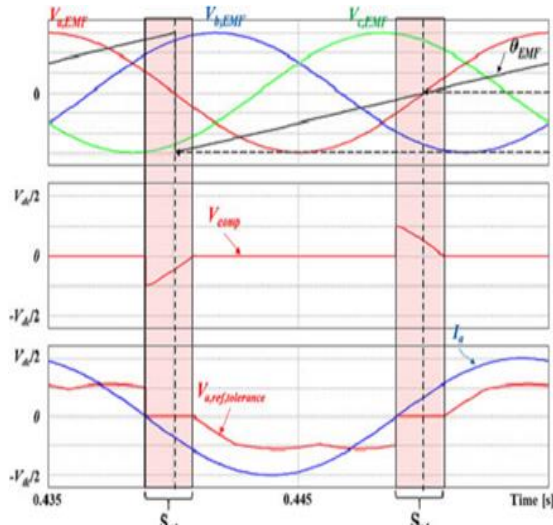


Fig. 8. Proposed tolerant control considering neutral-point voltage balance under the Sa1 open-circuit fault.

TABLE III

Principle Of The proposed tolerant control depending On The Position Of The open-Circuit fault

Position of open-circuit fault	V_{comp}	Compensation range
S_{a1} or S_{a4}	$-V_{a,ref,offset}$	$(0^\circ - \varphi_{pf}) \sim (0^\circ + \varphi_Z)$
S_{c4} or S_{c1}	$-V_{c,ref,offset}$	$(60^\circ - \varphi_{pf}) \sim (60^\circ + \varphi_Z)$
S_{b1} or S_{b4}	$-V_{b,ref,offset}$	$(120^\circ - \varphi_{pf}) \sim (120^\circ + \varphi_Z)$
S_{a4} or S_{a1}	$-V_{a,ref,offset}$	$(180^\circ - \varphi_{pf}) \sim (180^\circ + \varphi_Z)$
S_{c1} or S_{c4}	$-V_{c,ref,offset}$	$(240^\circ - \varphi_{pf}) \sim (240^\circ + \varphi_Z)$
S_{b4} or S_{b1}	$-V_{b,ref,offset}$	$(300^\circ - \varphi_{pf}) \sim (300^\circ + \varphi_Z)$

C. Considering Neutral-Point Voltage Balance

The compensation voltage which is one of the offset voltages can cause neutral-point voltage unbalance because V_{comp} calculated from (4) is a one-sided voltage [10], [24]. Therefore, two dc-link capacitors have different values depending on the polarity of V_{comp} generated for the open-circuit fault. The neutral-point voltage unbalance increases the voltage stress on the switch and the current THD [24]. The proposed tolerant control for the open-circuit fault of the outer switches has to incorporate a solution for the neutralpoint voltage unbalance problem.

Therefore, as mentioned earlier, V_{comp} is added for the corresponding compensation position depending on the position of the open-circuit fault, and then, V_{comp} is also added in the diametrically opposite compensation position to balance the neutral-point voltage. Fig. 8 shows the concept of proposed tolerant control considering the neutral-point voltage balance when the Sa1 open-circuit fault occurs. In Fig. 8, V_{comp} is added for the compensation range $[(0^\circ - \varphi_{pf}) \sim (0^\circ + \varphi_Z)]$ which corresponds to the position for the Sa1 open-circuit fault; in addition, V_{comp} is also added for the diametrically opposite compensation range $[(180^\circ - \varphi_{pf}) \sim (180^\circ + \varphi_Z)]$, which is the range for the Sa4 open-circuit fault. Two V_{comps} added in two positions have opposite polarity, and this results in the balanced neutral-point voltage. The final principles of the proposed tolerant control with the neutral-point voltage balance are summarized in Table III.

Fig. 9 shows $V_{x,ref,tolerance}$ and V_{comp} of the proposed tolerant control depending on the pf when M_a is 0.5. In Fig. 9, V_{comp} leads to $V_{a,ref,tolerance}$ with zero value in the corresponding compensation range. Moreover, the peak value of $V_{c,ref,tolerance}$ increases owing to V_{comp} .

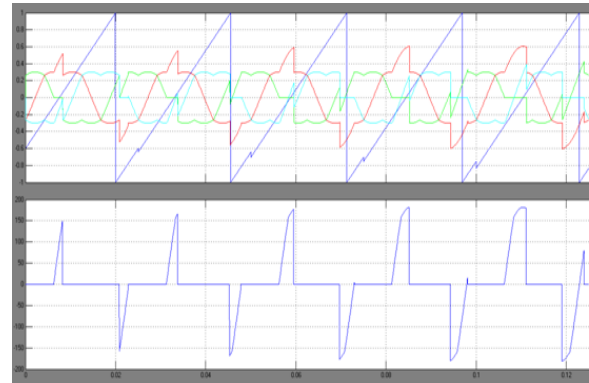


Fig. 9. $V_{x,ref,tolerance}(x=a,b,c)$ and V_{comp} depending on the pf when M_a is 0.5.

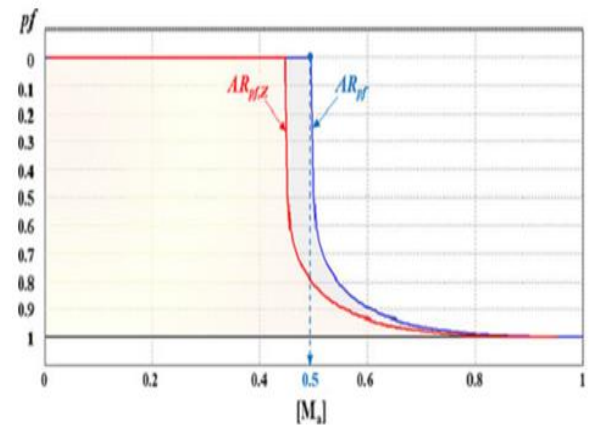


Fig. 10. Applicable range of the proposed tolerant control depending on M_a .

D. Limitation of Proposed Tolerant Control

$V_{x,ref,tolerance}$ cannot exceed a limitation voltage (V_{limit}) which is restricted by the dc-link voltage (V_{dc}). Therefore, V_{comp} is limited as follows

$$V_{comp} < V_{limit} - V_{ref,max} \quad (9)$$

Where V_{limit} is $V_{dc}/2$. On the basis of (9), the applicable operation range of the proposed tolerant control is determined depending on M_a and the pf . Fig. 9 shows $V_{x,ref,tolerance}$ and V_{comp} of the proposed tolerant control depending on the pf when M_a is 0.5. In Fig. 9, V_{comp} leads to $V_{a,ref,tolerance}$ with zero value in the corresponding compensation range. Moreover, the peak value of $V_{c,ref,tolerance}$ increases owing to V_{comp} .

Fig. 10 shows the applicable range for various values of M_a . The shaded part of Fig. 10 represents the applicable operation range. The proposed tolerant control is feasible over the entire factor range when M_a is smaller than 0.5. By increasing M_a from 0.5, the applicable operation range decreases. In Fig 10.

Table I V
Ipmsg Parameters Insimulation

Rated power	2.5 MW
Number of pole	8
Rated voltage (line-to-line)	760 V _{rms}
Rated current	1902 A _{rms}
Rated speed	1650 rpm
Resistance	0.4567 mΩ
q-inductance	0.0982 mH
d-inductance	0.0725 mH

Table V
Currentthdandrms Valuescomparison(600rpm,0.95pf)

	Normal (p.u.)	S_{a1} open-circuit fault	The proposed tolerant control
a-	5.4%, 1.51 kA _{rms}	14.8%, 1.49 kA _{rms}	6.1%, 1.51 kA _{rms}
b-	5.4%, 1.51 kA _{rms}	9.4%, 1.47 kA _{rms}	5.5%, 1.51 kA _{rms}
c-	5.4%, 1.51 kA _{rms}	8.1%, 1.55 kA _{rms}	6.0%, 1.51 kA _{rms}

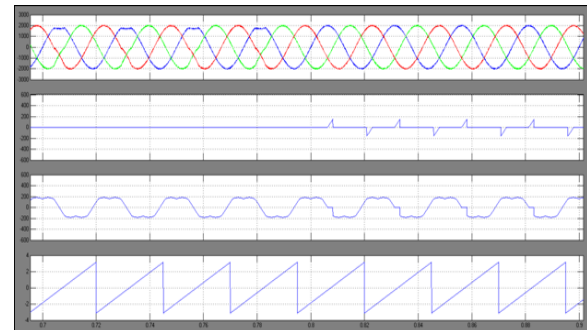
the applicable operation range shown as AR_{pf} is largest when only the p_{rel} related to ϕ_{pf} is taken into account. However, a large ϕ_Z means that large portion of the compensation range is reserved for ϕ_Z , and the rest can be used to compensate ϕ_{pf} . Therefore, ϕ_Z caused by the impedance of the PMSG reduces the applicable p_{rel} range, and it is shown in $AR_{pf,Z}$ with $\phi_Z=10$. ϕ_Z is determined by the operation conditions and parameters of the PMSG shown in (6). The proposed tolerant control has a limitation on its operation range that depends on the p_{rel} and M_a . However, considering that wind turbine systems do not always operate with the rated wind speed (high M_a) and that the operating p_{rel} of the rectifier with an IPMSG is not too low, the proposed tolerant control can clearly be effective.

IV. SIMULATION RESULTS

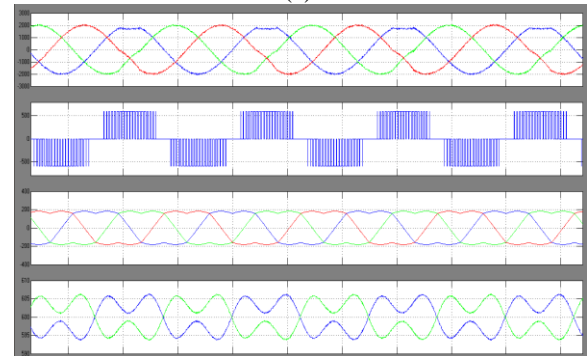
The simulation is performed using the PSIM tool. The 3L-NPC rectifier of the back-to-back converter with 2.5-MW IPMSG is only considered in the simulation. The IPMSG parameters used in the simulation are shown in Table IV. The proposed

tolerant control for the open-circuit fault of the outer switches (S_{x1}, S_{x4}) is implemented for different p_{rel} and generator speeds. Fig. 11 shows the simulation results of the proposed tolerant control when the S_{a1} open-circuit fault occurs. The speed of the PMSG is 600 rpm, M_a is 0.35, and the p_{rel} of the rectifier is 0.95. Owing to the S_{a1} open-circuit fault, the negative current is distorted as shown in Fig. 11(a). After the proposed tolerant control is applied, the reference voltages are changed by V_{comp} for the corresponding ranges $[(0 \text{ } \phi_{pf}) \sim (0 \text{ } \phi_Z), (180 \text{ } \phi_{pf}) \sim (180 \text{ } \phi_Z)]$ which are defined in Table III. As a result, the a-phase pole voltage (V_{an}) is clamped to 0 at their ranges as shown in Fig. 11(b) and the current distortion is eliminated completely.

In addition, the two dc-link capacitor voltages are balanced. The proposed tolerant control is effective for the p_{rel} transition operation of the rectifier. Fig. 12 shows the results when the proposed tolerant control is applied and the p_{rel} is changed from 0.95 to 0.9. The compensation range is extended as much as the p_{rel} decreases and the currents are maintained without distortion continuously. Moreover, we know that the peak value of $V_{c,ref,tolerance}$ becomes large because the p_{rel} decreases which was discussed in Section III.



(a)



(b)

Fig. 11. Simulation results with the proposed tolerant control under the S_{a1} open-circuit fault (600 rpm, $M_a=0.35, 0.95pf$).

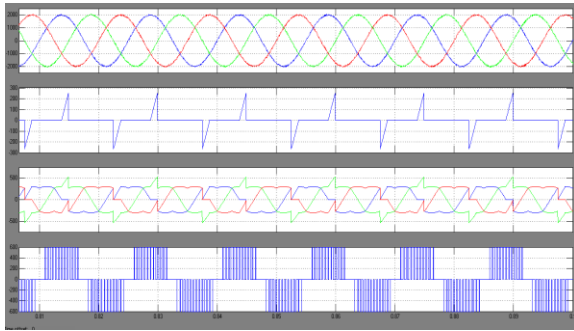


Fig. 12. Simulation results with the proposed tolerant control under the Sa1 open-circuit fault (600 rpm, $Ma = -0.35$, pf-transition from 0.95 to 0.9).

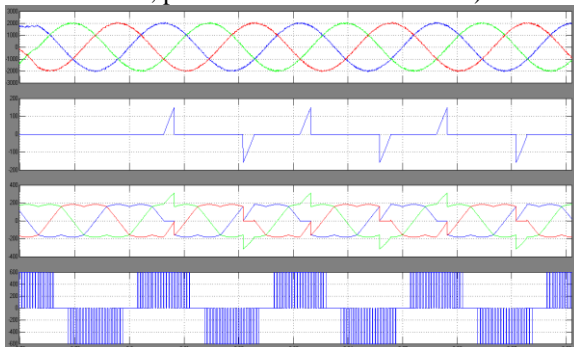


Fig. 13. Simulation results with the proposed tolerant control under the Sa1 open-circuit fault (1000 rpm, $Ma = 0.59$, 0.95pf)

Fig. 13 shows the performance of the proposed tolerant control under the Sa1 open-circuit fault at different speed (1000 rpm) of the PMSG when Ma is 0.59. Similar to Fig. 11, the distorted currents are corrected after the proposed tolerant control is applied. However, the peak value of $V_{c,ref,tolerance}$ is close to $V_{limit}(V_{dc}/2)$ at 0.95pf, which is different from what is shown in Fig. 11. This is because Ma of Fig. 13 has a smaller applicable operation range than that of Fig. 11, which can be seen in Fig. 10. Table V shows the current THD results before and after the proposed tolerant control is applied. The current THD is increased by the Sa1 open-circuit fault; however, owing to the proposed tolerant control, the current THD is restored as good as normal state without any open-circuit fault.

VI. CONCLUSION

According to the paper which is developed the tolerant control for the open-circuit fault of the outer switches in three-level rectifiers (both 3L-NPC and T-type topologies) which is utilized in the wind turbine systems. According to the basis of the analysis of the tolerant control for each open-circuit fault which is proposed about the neutral-point voltage balance. Moreover according to the control

system which is implemented by adding a compensation voltage (V_{comp}) to the reference voltages for the corresponding compensation ranges depending on the position of the open-circuit fault. From the fig :10 we can analysis the control which is used in both the 3L-NPC and T-type rectifiers and guaranting during the normal operation without a change of the pf in the applicable operation range which is depend upon the modulation index (Ma) and the pf. By using the simulation result we can analysis the performance of the proposed system.

REFERENCES

- [1] A. Isidori, F. M. Rossi, F. Blaabjerg, and K. Ma, "Thermal loading and reliability of 10-MW multilevel wind power converter at different wind roughness classes," *IEEE Trans. Ind. Appl.*, vol. 50, no. 1, pp. 484–494, Jan./Feb. 2014.
- [2] H. G. Jeong, K. B. Lee, S. Chio, and W. Choi, "Performance improvement of LCL-filter-based grid-connected inverters using PQR power transformation," *IEEE Trans. Power Electron.*, vol. 25, no. 5, pp. 1320–1330, May 2010.
- [3] S. Li, T. A. Haskew, R. P. Swatloski, and W. Gathings, "Optimal and direct-current vector control of direct-driven PMSG wind turbines," *IEEE Trans. Power Electron.*, vol. 27, no. 5, pp. 2325–2337, May 2012.
- [4] W. Qiao, L. Qu, and R. G. Harley, "Control of IPM synchronous generator for maximum wind power generation considering magnetic saturation," *IEEE Trans. Ind. Appl.*, vol. 45, no. 3, pp. 1095–1105, May/June 2009.
- [5] S. Morimoto, H. Nakayama, M. Sanada, and Y. Takeda, "Sensorless output maximization control for variable-speed wind generation system using IPMSG," *IEEE Trans. Ind. Appl.*, vol. 41, no. 1, pp. 60–67, Jan./Feb. 2005.
- [6] Y. Zhao, W. Qiao, and L. Wu, "An adaptive quasi-sliding-mode rotor position observer-based sensorless control for interior permanent magnet synchronous machines," *IEEE Trans. Power Electron.*, vol. 28, no. 12, pp. 5618–5629, Dec. 2013.
- [7] P. B. Reddy, A. M. EL-Refaei, and K. K. Huh, "Effect of number of layers on performance of fractional-slot concentrated-windings interior permanent magnet machines," *IEEE Trans. Power Electron.*, vol. 30, no. 4, pp. 2205–2218, Apr. 2015.